JPET Fast Forward. Published on December 14, 2010 as DOI: 10.1124/jpet.110.175752

JPET #175752

PHARMACOKINETIC AND PHARMACODYNAMIC MODELING OF EXENDIN-4 IN TYPE 2 DIABETIC GOTO-KAKIZAKI RATS

WEI GAO AND WILLIAM J. JUSKO

Department of Pharmaceutical Sciences, State University of New York at Buffalo, Buffalo, New York, 14260.

a) Running Title: PK/PD modeling of Exendin-4 in Goto-Kakizaki rats

b) Corresponding author: William J. Jusko, 565 Hochstetter Hall, Department of Pharmaceutical Sciences, University at Buffalo, State University of New York. Buffalo, New York 14260

Phone: 716-645-2855

Fax: 716-645-3693

Email: wjjusko@buffalo.edu

c) Text pages: 21

Tables: 2

Figures: 7

References: 39

Words in Abstract: 212

Words in Introduction: 469

Words in Discussion: 1418

d) Abbreviations: GK: Goto-Kakizaki; TMDD: target-mediated drug disposition; PK: pharmacokinetics; PD: pharmacodynamics; GLP-1: glucagon-like peptide-1; GLP-1R: GLP-1 receptor.

e) Recommended section: Endocrine and Diabetes

Abstract

The pharmacokinetics (PK) and pharmacodynamics (PD) of exendin-4 were studied in type 2 diabetic Goto-Kakizaki (GK) rats after single doses at 0.5, 1, 5 or 10 μg/kg by intravenous (iv) and 5 μg/kg by subcutaneous (sc) administration. Plasma exendin-4, glucose, and insulin concentrations were determined. A target-mediated drug disposition (TMDD) model was used to characterize the PK of exendin-4. Glucose turnover was described by an indirect response model, with insulin stimulating glucose disposition. Insulin turnover was characterized by an indirect response model with a precursor compartment. After iv doses, exendin-4 rapidly disappeared from the circulation, while it exhibited rapid absorption (T_{max} = 15-20 min) and incomplete bioavailability (F = 0.51) after the sc dose. Exendin-4 increased insulin release at 2 to 5 min with capacity S_{max} = 6.91 and sensitivity SC_{50} = 1.29 nmol/L, followed by a rebound at 10 to 15 min and a slow return to the baseline. Glucose initially declined due to enhanced insulin secretion, and then gradually increased due to the activation of the neural system by exendin-4. The hyperglycemic action was modeled with increased hepatic glucose production with a linear factor S_{RC} = 0.112 L/nmol. The mechanistic PK/PD model satisfactorily described the disposition and effects of exendin-4 on glucose and insulin homeostasis in type 2 diabetic rats.

Introduction

Exendin-4 is a 39 amino acid glucagon-like peptide-1 (GLP-1) analog, which was found originally in the saliva of the gila monster. It shares approximately 53% sequence homology with the mammalian GLP-1 (Doyle and Egan, 2007). Due to amino acid changes, exendin-4 is resistant to the degradation of the enzyme dipeptidyl peptidase-4 (DPP-4), and has a longer half-life than native GLP-1. Exendin-4 binds to GLP-1 receptors (GLP-1R) to exhibit anti-diabetic actions, including glucose-dependent stimulation of insulin secretion, delay of gastric emptying, and protection of beta-cells. Twice-daily administration has been associated with improvements in glycemic control in type 2 diabetic subjects that are inadequately treated with existing antidiabetic agents (Cvetkovic and Plosker, 2007). Single bolus doses of exendin-4 effectively reduced postprandial plasma glucose excursions in man (Kolterman et al., 2005). Long term treatment has been shown to lower HbA1c, to decrease body weight, and to improve beta-cell function in animals and humans (Young et al., 1999; Tourrel et al., 2002; Klonoff et al., 2008).

The GK rats, a lean model of type 2 diabetes, exhibit spontaneous polygenic disease (Goto et al., 1988). This is produced by repeated inbreeding of Wistar rats using glucose intolerance as the selection index. After 35 generations of breeding, diabetes in this animal model is stable. The GK rat shows hyperglycemia, mild insulin resistance, impaired glucose-induced insulin secretion, and a decrease of β cell mass. Exendin-4 has shown promising anti-diabetic effects in GK rats. Tourrel et al. (Tourrel et al., 2002) observed an expansion of beta-cell mass and a delay of the onset of overt

diabetes in the GK rats after 5 days of exendin-4 treatment during the neonatal age. Furthermore, 12 weeks of treatment from 10 weeks of age effectively decreased HbA1c in GK rats (Simonsen et al., 2009).

Mechanism-based pharmacokinetic/pharmacodynamic (PK/PD) models can be used to quantitatively understand the relationship between drug concentrations (PK) and biological responses (Mager et al., 2003). Extensive PK/PD modeling was applied to characterize the glucose and insulin system in various circumstances, such as for the glucose tolerance test or during drug treatment (Landersdorfer and Jusko, 2008; Silber et al., 2010). However, the only currently available PD model for exendin-4 was proposed by Mager et al (Mager et al., 2004). The model characterized the effects of exendin-4 on human glucose-insulin homeostasis in hyperglycemic clamp studies, but used a hypothetical linear PK function.

Based on the promising antidiabetic effects of chronic exendin-4 treatment, we aimed to investigate the immediate effects after acute administration in diabetic GK rats. Further understanding of the role of exendin-4 on the regulation of the glucose and insulin system was assessed using extensive experimental data obtained from GK rats and mechanistic PK/PD modeling. The PK/PD model was further validated using separate animal studies. Utilizing rats as an experimental model to assess the PD of exendin-4 was also addressed.

Methods and Materials

Animals

All studies were approved by the Institutional Animal Care and Use Committee of the University at Buffalo. Male Goto-Kakizaki rats at 9-10 weeks with weights ranging from 200-250 g were purchased from Taconic Farms (Germantown, NY). The animals had free access to food and water and were maintained on a 12/12-h light/dark cycle. All animals were acclimatized for 1 week before the initiation of the study. One day prior to the study, all rats underwent right jugular vein cannulation under ketamine/xylazine anesthesia. Cannula patency was maintained with sterile 0.9% saline.

Experimental

Exendin-4 (GenScript USA Inc., Piscataway, NJ) was diluted immediately before injection using saline for injection. Rats were divided into five groups (0.5, 1, 5 or 10 µg/kg by iv and 5 µg/kg by sc doses) on the basis of equivalent mean values of glucose and body weight (n = 3 for 0.5 µg/kg, n = 6 for 1 ug/kg, n = 5 for 5 ug/kg, n = 7 for 10 ug/kg and n = 6 for 5 ug/kg, sc). Sampling times were selected based on previous pilot studies of exendin-4 PK and dynamic effects. Plasma was stored at -80°C until assay. The blood volume taken was less than 0.9% of body weight.

Plasma concentrations of exendin-4 were determined using the commercial Exendin-4 EIA kit (Phoenix Pharmaceuticals, Inc., Burlingame, CA). Standard curves ranged from 0 to100 ng/ml, and the linear range was from 0.08 to 0.86 ng/ml. The lower limit of detection was 0.08 ng/ml, and the lower limit of quantification was 0.1 ng/ml. The intra-assay variability was <10% and the inter-assay variability was <15%. Plasma

samples with exendin-4 concentrations >0.86 ng/ml were diluted with the diluents provided by the manufacturer. General procedures followed the manufacturer's instructions. Plates were read at OD450 on a SpectraMax 190 ELISA plate reader (Molecular Devices, Sunnyvale, CA).

Blood glucose was measured using a BD Logic blood glucose meter (BD Medical, Franklin Lakes, NJ). Plasma insulin was measured using a commercial rat ELISA kit (Millipore Corporation, St. Charles, MO). The assay was carried out according to manufacturer's directions with the coefficient of variation between assays of <10%.

Model Evaluation Animal Studies

Study 1 was conducted in 3 GK rats (10.5 weeks old). After recovery from cannulation surgery, rats received exendin-4 (5 μg/kg) through the cannula. Blood glucose was monitored within 2 hours. After two days of wash-out, rats were given the drug at the same dose level, and insulin concentrations were measured.

Study 2 was conducted in 2 GK rats (11 weeks old). After recovery from jugular vein cannulation, rats were dosed with exendin-4 (5 μg/kg) via sc injection. Blood glucose and insulin were measured.

PK/PD Model

For initial PK data evaluation, mean profiles of exendin-4 for each iv dose obtained from rats were used to perform a noncompartmental analysis (NCA) and curve fitting to a biexponential equation ($C_p = C_1 \cdot e^{-\lambda 1 \cdot t} + C_2 \cdot e^{-\lambda 2 \cdot t}$) using WinNonlin 5.0 (Pharsight Corp., NC) to evaluate dose-dependent changes in clearance (*CL*), central (V_c) and steady-state volumes of distribution (V_{ss}), and distributional clearance (CL_D).

JPET Fast Forward. Published on December 14, 2010 as DOI: 10.1124/jpet.110.175752
This article has not been copyedited and formatted. The final version may differ from this version.

For the next stage, a mechanism-based modeling approach was used for data analysis. The general scheme of the applied PK/PD model is presented in Figure 1. The free exendin-4 (C) in plasma can bind to GLP-1R (R) with a second-order rate constant (k_{on}) to form drug-receptor complex (RC), distribute to and from tissues (A_T) by first-order rates (k_{pt} and k_{tp}), and be directly eliminated (k_{el}). The RC can dissociate at a first-order rate (k_{off}) and be internalized and degraded (k_{int}). The GLP-1R (R) is synthesized at a zero-order rate (k_{syn}) and degraded at a first-order rate (k_{deg}) with the relationship of $R_{tot} = k_{syn}/k_{deg}$. The TMDD PK model can be described by:

$$\frac{dC}{dt} = Input(t) - (k_{el} + k_{pt}) \cdot C + k_{tp} \cdot A_T/V_C - k_{on} \cdot R \cdot C + k_{off} \cdot RC; \qquad \text{Eq.1}$$
$$C(0) = Dose/V_C (iv) \text{ or } 0 \text{ (sc)}$$

$$\frac{dA_T}{dt} = k_{pt} \cdot C \cdot V_C - k_{tp} \cdot A_T; \qquad A_T(0) = 0 \qquad \text{Eq. 2}$$

$$\frac{dR}{dt} = k_{syn} - k_{on} \cdot R \cdot C + k_{off} \cdot RC - k_{deg} \cdot R; \qquad R(0) = R_{tot} \qquad \text{Eq. 3}$$

$$\frac{dRC}{dt} = k_{on} \cdot R \cdot C - (k_{off} + k_{int}) \cdot RC; \qquad RC(0) = 0 \qquad \text{Eq. 4}$$

The input function for Eq.1 following iv doses is 0, and following sc doses is:

$$Input(t) = k_a \cdot F \cdot Dose \cdot exp(-k_a \cdot t)/V_C \qquad \text{Eq. 5}$$

where k_a is the first-order absorption rate constant and F is the absolute bioavailability after sc doses. Units for C, R and RC are nmol/L, and those for other parameters are listed in Table 1.

Pharmacodynamic Model

The pharmacodynamic model proposed for insulintropic effects of exendin-4 is shown in Figure 1. Blood glucose arises from exogenous food intake and endogenous gluconeogenesis and glycogen breakdown. It can be consumed for energy or stored as glycogen or fat in peripheral tissues. In animals with normal β-cell function, once glucose concentrations rise, it will be transported into β-cells to stimulate insulin synthesis and release. Insulin has broad glucose-lowering effects by inhibiting inputs such as gluconeogenesis and glycogenolysis, as well as by stimulating outputs such as glucose uptake into peripheral tissues, glycogen synthesis, triglyceride synthesis and storage. This metabolic system is maintained in balance in normal physiological states. However, glucose appeared not to stimulate insulin release efficiently in GK rats. After the rapid release during the initial phase (0-10 min), insulin response was blunted even though glucose was much higher than basal levels (Edholm et al., 2009).

Exendin-4 has direct effects on hepatic glucose production and it stimulates glucose increase through activation of the neural system (Perez-Tilve et al., 2010). The hyperglycemic effect lasted longer than insulin release, and a biophase compartment could be utilized to describe the delay. However, the decline of glucose during the later time of the study period occurs in parallel with RC profiles and a biophase compartment generated profiles with similar trends as RC. Therefore, RC acts similarly to a biophase compartment and was used as the driving function for the glucose elevation.

Based on the above mechanisms, a PD model incorporating glucose/insulin inter-regulations as well as exendin-4 effect on glucose and insulin was developed as

depicted in Figure 1. The model equations were fitted to glucose and insulin data from all treatments simultaneously.

Glucose homeostasis was described by an indirect response model: k_{outG} is the first-order output rate constant, and k_{inG} is the zero-order input rate constant. The dynamics of insulin was characterized by an indirect response model with a precursor pool: k_0 is the zero-order precursor input rate constant, and k_p and k_{outI} are the first-order precursor and insulin output rate constants with the relationship $k_0 = k_p \cdot InsP_0 = k_{outI} \cdot Ins_0$, where $InsP_0$ and Ins_0 are the precursor and insulin concentrations before treatment. Insulin stimulates glucose disposition with a linear stimulation factor S_{Ins}. The change of insulin from its threshold value (Ins_h) was used to drive this stimulatory effect.

Exendin-4 stimulated the precursor pool to release insulin via C and glucose production via RC. The glucose and insulin changes are described by:

$$\frac{dGlu}{dt} = k_{inG} \cdot (1 + S_{RC} \cdot RC) - k_{outG} \cdot (1 + S_{Ins} \cdot (Ins - Ins_h)) \cdot Glu \quad \text{Eq. 6}$$
$$with\ Glu(0) = Glu_0 = k_{inG} / k_{outG} \cdot (1 + S_{Ins} \cdot (Ins_0 - Ins_h))$$

$$\frac{dInsP}{dt} = k_0 - k_p \cdot InsP \cdot (1 + \frac{S_{max} \cdot C}{C + SC_{50}}) \quad \text{Eq.7}$$
$$with\ InsP(0) = InsP_0$$

$$\frac{dIns}{dt} = k_p \cdot InsP \cdot (1 + \frac{S_{max} \cdot C}{C + SC_{50}}) - k_{outI} \cdot Ins \quad \text{Eq. 8}$$
$$with\ Ins(0) = Ins_0$$

where S_{max} and SC_{50} are drug-specific parameters representing the maximum stimulation of the response and the exendin-4 concentration required for half-maximum stimulation. The threshold insulin Ins_h is fixed as the literature value of 1.44 ng/ml (Gao

et al., 2007). The unit of *Glu* is mg/dL and the unit of *InsP* and *Ins* is ng/ml. The units of individual PD parameter are listed in Table 2.

Naïve-pooled data from all animals in each dose group were used to fit the PK/PD model. The PK samples below the limit of quantifications were discarded. All computer fittings and simulations were done using ADAPT II (BMSR, USC, CA) with the maximum likelihood method (D'Argenio and Schumitzky, 1997). The variance model was $V_i = (\sigma_1 + \sigma_2 \cdot \hat{Y})^2$ where V_i is the variance of the i^{th} data point, σ_1 and σ_2 are the variance model parameters, and $\hat{Y}_i$ represents the i^{th} model predicted value.

Various proposed PD models were fitted and compared, including models containing glucose-induced insulin release and exendin-4-induced precursor synthesis or inhibiting glucose output. The PK model was compared with the Michaelis-Menten (MM) model. The final model was selected based on visual inspection of curve fitting, estimator criterion value, sum of squared residuals, Akaike information criterion, and confidence of parameter estimations. After development of the PK/PD model, simulations were overlaid with observations from the confirmatory animal studies. Only the final model fitting results are presented.

Results

Pharmacokinetics

One objective of this study was to evaluate the PK of exendin-4 in GK rats. The mean exendin-4 concentration-time profiles after various doses in rats are shown in Figure 2. The PK profiles show a biexponential decline with typical characteristics of TMDD where low doses showed rapid decline in early concentrations after iv injection. Terminal half-lives ranged from 15 to 33 min with increasing doses following iv injection. The NCA results from the mean profiles of exendin-4 are summarized in Figure 3. Due to limited target binding capacity, drugs exhibiting TMDD often show saturable clearance and distribution, with decrease in apparent distribution parameters (CL, CL_D and V_{ss}) with increasing doses. Generally, this trend is not observed with the central compartment volume, V_c. However, GLP-1Rs are widely expressed in vivo and these receptors may occupy tissues which are in rapid equilibrium with blood resulting in changes in V_c. After sc injection, the terminal half-life was 70 min, indicating the involvement of slow absorption and flip-flop kinetics.

The proposed PK model well captured the overall profiles of exendin-4 after both routes of administration at each dose level as shown in Figure 2. A Michaelis-Menton (MM) model is the most common model dealing with saturation kinetics. However, even with fewer parameters, this model did not provide a better fitting than the TMDD model. Moreover, the MM model lacks a complete mechanistic nature and does not include the endocytosis process that is initiated upon binding of exendin-4 to GLP-1R. Thus, considering that no overparameterization existed in this case (Gibiansky et al., 2008),

the better model fittings and description of the underlying mechanisms of exendin-4 disposition justifies preference of the TMDD model.

All parameters were estimated (Table 2) with reasonable precision (< 40% except for k_{pt}). The clearance ($CL_c = k_{el} \cdot V_c$) is 8.6 ml/min/kg. In GK rats, the relative contribution of CL_c to the total clearance was only 20% at the lowest dose, and nearly 100% at the highest doses. The equilibrium dissociation constant K_D (= k_{off}/k_{on} = 0.19 nM) is in the range of the reported values for specific binding of exendin-4 and GLP-1 to normal rat tissues (Goke et al., 1995; Larsen et al., 1997; Satoh et al., 2000).The total receptor (R_{tot}) was estimated to be 5.17 nmol/L for GK rats. The internalization rate in GK rats was lower than k_{el}. After sc injection, bioavailability was estimated to be 50.7.

Pharmacodynamics

Changes of insulin and glucose concentrations after exendin-4 injection in GK rats are shown in Figure 4. Baseline insulin was 3.75 ± 1.32 ng/ml (p = 0.17 between groups). Plasma insulin markedly increased in all dose groups and reached a maximum at 2 min for all iv dose groups, and at 5 min for the sc group. The peak insulin concentrations were not significantly different (p = 0.11). At around 10 min, the insulin profiles showed a rebound as concentrations went below baseline and slowly returned to the pre-treatment value. Insulin responses in the high dose group were significantly higher than the lowest dose group ($AUC_{ins(0\text{-}8min)}$ above baseline $p < 0.05$). A trend of a sigmoidal dose response relationship existed, but was not significant.

The average glucose concentration was 267 ± 59 mg/dL, and not different between groups (p = 0.63). After 0.5 µg/kg exendin-4 injection, blood glucose

increased immediately from 229 mg/dL and peaked at 389 mg/dL at 20 min. All other groups had similar patterns: a transient drop after exendin-4 injection, and a gradual increase to the maximum at around 60 min, followed by a slow decline at similar rates. The percent glucose change over baseline at 20 min was significantly different between dose groups ($p = 0.03$).

As shown in Figure 4, the present integrated PK/PD model (Figure 1) adequately characterized glucose and insulin concentrations. Table 2 lists the parameter estimates. This model represented the final selection after comparing several other model versions. For example, the feedback model was initially fitted to the data, but it failed to describe the blunted insulin response in the late phase when glucose stayed high. Another model with exendin-4 stimulating insulin precursor production could not characterize the rapid increase and decline of insulin during the first time points. Glucose and insulin concentrations in all dose groups were captured nicely with the current PK/PD model. Moreover, the model successfully predicted the insulin and glucose responses in studies conducted in separate groups of animals (Figure 5). In the confirmatory animal studies, the two groups of rats came from different batches and the sampling schedules were different. The model predictions reasonably agree with the observed responses.

Parameters controlling glucose and insulin metabolism were estimated with good precision (<80%) and comparable to literature reported values. The k_{outI} was identical to the one observed in SD rats (unpublished data), although the simple indirect response model was used to describe insulin turnover in SD rats. The k_{out} value for glucose was 0.0224 min^{-1}, corresponding to a half-life of 31 min. The k_{outG} was only half of that in SD

rats, suggesting the acute insulin-independent glucose utilization in GK rats might be impaired. Baseline parameters Glu_0 and Ins_0 were estimated separately for each dose group to account for the high variability of glucose and insulin concentrations. This resulted in different parameter values for the glucose production rate constant (k_{inG}), insulin precursor production rate constant (k_{0I}) and insulin precursor levels ($InsP_0$), but otherwise the profiles were fitted with a universal set of parameters. Parameter S_{Ins} (0.708 ml/ng) describes the regulation of glucose disposition by insulin in GK rats. It implies that glucose utilization would increase 2-fold when insulin concentrations increase by 1.4 ng/ml.

The S_{max} and SC_{50} are drug-specific parameters characterizing exendin-4 effects on insulin regulation. Both the plasma drug concentration (C) and the drug-receptor complex (RC) were tested as the driving force for insulintropic effect, with the former favored. The straightforward evidence is that, after iv bolus of exendin-4, the maximum insulin stimulation occurred prior to the maximum *RC*. Actually, pancreatic GLP-1R is mostly expressed on the surface of the beta cells facing the endothelium (Tornehave et al., 2008), exendin-4 can bind to receptors quite fast and can directly stimulate insulin release. Therefore, a biophase compartment between plasma and pancreas is unnecessary. The current study confirms that the plasma concentration (C) is a more appropriate driving force for exendin-4 to stimulate insulin release. In the two high dose groups, plasma exendin-4 concentrations were maintained above its SC_{50} (1.29 nmol) for 30-45 min after injection, which leads to the delayed insulin return to baseline from the rebound.

Glucose profiles declined during the late phase of the study in parallel with each other and with a rate close to the decreasing rate of the exendin-4-GLP-1R complex (*RC*) (Figure 6). A biophase between *C* and SG_{max} was unnecessary since the biophase profiles showed similar trends with *RC*. Therefore, *RC* was used to drive hyperglycemia by enhancing glucose production via the activation of the neural system (Perez-Tilve et al., 2010), with a linear stimulation factor estimated to be 0.112. A sigmoidal model was examined, but resulted in a SD_{50} with low precision (CV = 1720%) and a higher AIC value. Therefore, the linear model was used. Due to slow turnover of *RC*, this hyperglycemic effect was prolonged for 300 to 900 min.

Discussion

Exendin-4 shows anti-diabetic effects in animals and humans. To our knowledge, this is the first study of the acute effects of exendin-4 in diabetic rats with application of a mechanistic model to quantify its disposition and acute effects on glucose-insulin homeostasis. A general TMDD model delineating receptor-mediated drug disposition was proposed to characterize the nonlinear kinetics. The likely mechanism of action of exendin-4 was integrated into a model of the glucose-insulin system, thereby facilitating the simultaneous analysis of glucose and insulin responses to drug effects.

Pharmacokinetics

A general TMDD approach to model in vivo PK data of drugs was introduced and successfully applied to many different therapeutic agents (Mager and Jusko, 2001). In GK rats, all concentration profiles from 5 dose levels (Figure 2) were well described with one set of PK parameters using the TMDD model.

A wide range of doses is needed to detect and properly quantify nonlinearities in PK. In this study, the dose was as low as 0.5 μg/kg. Early concentration data were available from 2 min after iv bolus dosing, and observed concentrations ranged widely around the K_D value. Therefore, all parameters were precisely estimated.

The primary elimination route of exendin-4 has been proposed as glomerular filtration (Copley et al., 2006) and, physiologically, k_{el} represents elimination by kidney. The CL_c in GK rats was similar to reported creatinine clearances in GK rats (Sato et al., 2003). Renal function appears to be similar between GK and healthy rats at the age when the current study was conducted (Phillips et al., 1999; Schrijvers et al., 2004). In

JPET Fast Forward. Published on December 14, 2010 as DOI: 10.1124/jpet.110.175752
This article has not been copyedited and formatted. The final version may differ from this version.

addition, clearance was only slightly reduced in patients with mild to moderate renal impairment (Linnebjerg et al., 2007).

The GLP-1R goes through endocytosis and, in the presence of agonist, the receptor cycles between the plasma membrane and endosomal compartment. The internalization of rat GLP-1R was examined in cell lines, with k_{on} as 0.082 L/min.nmol and k_{off} as 0.015 and 0.21 min^{-1} (Widmann et al., 1995). Interestingly, our estimated k_{on} was very similar to the measured value, and k_{off} was identical to the lower value, which resulted in a K_D similar to the reported lower value and comparable with other findings (Goke et al., 1995; Larsen et al., 1997; Satoh et al., 2000). Total receptor concentrations at steady-state (R_{tot}) in GK rats exhibited a turnover half-life of 40 min.

Pharmacodynamics

A mechanistic PK/PD model was developed to jointly describe the insulintropic effect of exendin-4 and its regulation on glycemic control in GK rats.

We found that exendin-4 produced insulin release immediately after bolus administration in a dose-dependent manner in GK rats. The acute insulintropic effect was modeled as the direct action on the insulin release rate, similar to a model in humans (Mager et al., 2004).

As previously found in Wistar rats (Greig et al., 1999), after exendin-4 treatment, a rebound phenomenon was observed. After a rapid release during the early time points, insulin concentrations fell below basal concentrations at 15 min and slowly returned to baseline. Moreover, in the pancreas perfusion study, GK rats exhibited a marked early

response (<10 min) to GLP-1, but a blunted late phase response, even when glucose was 5-fold higher (Edholm et al., 2009).

Models that describe PD adaptation processes have been introduced on the basis of their primary mechanism (Mager et al., 2003). For the rebound phenomenon observed in our data, one possible mechanism could be precursor pool depletion (Sharma et al., 1998). Insulin secretion and release from beta cells consists of a series of compartments: readily released, newly synthesized, and the release pool which can be depleted by stimulation from exendin-4. It may take time to fill the depleted pool due to the slow synthesis rate. The duration of rebound depends on the administered dose (Figure 7). The precursor indirect response model successfully characterized insulin profiles in GK rats.

In the current study, the stimulation of insulin by exendin-4 in GK rats seems to be independent of glucose. This is possibly because chronic hyperglycemia already exists in GK rats, apart from the impaired glucose-stimulated insulin response. In addition, a TIFR imaging study (Ohara-Imaizumi et al., 2004) suggested that glucose rarely stimulated insulin release from docked granules in GK rats. Therefore, it appears valid to assume glucose is not involved in the stimulation caused by exendin-4.

Acute administration of exendin-4 has been shown to ameliorate hyperglycemia in animals by stimulating insulin secretion or directly promoting glucose metabolism (Vahl et al., 2007; Sandoval et al., 2008; Zheng et al., 2009). However, in rodents, most of these acute hypoglycemic effects have been found in mice studies (Young et al., 1999; Arakawa et al., 2009), and responses are less clear in rats.

In GK rats, after the transient decrease, glucose actually increased and remained at a high level until 2 hours. Similarly, several other groups have observed that acute administration of exendin-4 causes hyperglycemia in multiple strains of rats (Aziz et al., 2005; Perez-Tilve et al., 2010). Extensive studies showed that acute administration of exendin-4 only lowered the glycemic response to glucose challenge in the early phase as a result of augmented early insulin secretion, and then induced hyperglycemia dose-dependently 15-30 min after drug administration without further increased insulin response (Perez-Tilve et al., 2010). However, Parkes et al. (Parkes et al., 2001) did not observe a profound glucose response when infusing exendin-4 to SD rats. One of the possible reasons could be that the first observed time point in their study was 15 min, past the time frame when the immediate insulin release and hypoglycemia were obvious in GK rats. Moreover, the glucose concentrations in SD rats were not as high as in GK rats to initiate the initial hypoglycemic effect. In addition, the hyperglycemic effect might be hidden under the response caused by the iv glucose bolus given at 30 min after the start of exendin-4 infusion in SD rats.

The hyperglycemic effect was believed to be related to GLP-1R in the nervous system. After acute administration, exendin-4 enters either the peripheral circulation or the central nervous system and, by activating the sympathetic nervous system, it increased blood glucose likely through enhancing hepatic glucose production in rats (Perez-Tilve et al., 2010). Our results confirmed that acute administration of exendin-4 also involves some complexities in diabetic rats: exendin-4 regulates glucose in vivo by

stimulating its production (probably via nervous system stimulation) and by enhancing its utilization (via increased insulin secretion).

In the current PK/PD model, exendin-4 directly stimulates glucose production (k_{inG}). Due to the dual effects from exendin-4 and insulin, blood glucose will decrease and then increase to a high level after acute treatment. A high dose of exendin-4 can overcome the expected benefits on insulin and glucose metabolism (Figure 7) and lead to the initial glucose lowering effect to a lesser extent and a severe hyperglycemia in later time points. These results have important implications for the design and interpretation of studies using exendin-4 in diabetic rats. Although this hyperglycemic effect is not observed in humans, it might need further investigation whether it is related to the adverse effects of exendin-4 in diabetic patients.

The ability of exendin-4 to elevate blood glucose diminished over time in healthy rats (Perez-Tilve et al., 2010). We also found that the hyperglycemic effect is adaptable in GK rats and chronic exposure of exendin-4 by osmotic pump decreased blood glucose compared with saline treated controls (unpublished data), consistent with the beneficial glycemic effects from chronic administration in rats (Xu et al., 1999; Simonsen et al., 2007).

The GLP-1R exists in numerous tissues such as brain, pancreas, intestine and kidney. The present model assumes that all receptors are involved in the PK, although it is possible that differences in affinity or access exist among tissues. Total exendin-4-GLP-1R complex (*RC*) was used as the driving function for activation of the neural

system. A more physiological way is to include a fractional factor operating on *RC* as not all receptors or *RC* are involved in this effect.

In conclusion, we have demonstrated a novel aspect of exendin-4 action, acute hyperglycemia, in type 2 diabetic rats. Exendin-4 raises blood glucose even in the face of potentiated insulin secretion, and this action may result from increased hepatic glucose production. The mechanism-based PK/PD model well describes the PK profiles and the PD responses to both iv and sc doses of exendin-4 in GK rats. Our findings raise important considerations for investigating the acute glycemic effect of exendin-4 in diabetic rats, and whether those effects could be related to adverse effects of drugs in diabetic patients.

Authorship Contribution

Wei Gao enacted experiments and modeling and wrote manuscript.

William Jusko helped plan studies, advised on modeling, and revised manuscript.

References

Arakawa M, Ebato C, Mita T, Hirose T, Kawamori R, Fujitani Y and Watada H (2009) Effects of exendin-4 on glucose tolerance, insulin secretion, and beta-cell proliferation depend on treatment dose, treatment duration and meal contents. *Biochem Biophys Res Commun* **390**:809-814.

Aziz A, Anderson GH, Giacca A and Cho F (2005) Hyperglycemia after protein ingestion concurrent with injection of a GLP-1 receptor agonist in rats: a possible role for dietary peptides. *Am J Physiol Regul Integr Comp Physiol* **289**:R688-694.

Copley K, McCowen K, Hiles R, Nielsen LL, Young A and Parkes DG (2006) Investigation of exenatide elimination and its in vivo and in vitro degradation. *Curr Drug Metab* **7**:367-374.

Cvetkovic RS and Plosker GL (2007) Exenatide: a review of its use in patients with type 2 diabetes mellitus (as an adjunct to metformin and/or a sulfonylurea). *Drugs* **67**:935-954.

D'Argenio DZ and Schumitzky A (1997) ADAPT II user's guide: pharmacokinetic/pharmacodynamic system analysis software. Biomedical Simulations Resource, Los Angeles, CA.

Doyle ME and Egan JM (2007) Mechanisms of action of glucagon-like peptide 1 in the pancreas. *Pharmacol Ther* **113**:546-593.

Edholm T, Cejvan K, Abdel-Halim SM, Efendic S, Schmidt PT and Hellstrom PM (2009) The incretin hormones GIP and GLP-1 in diabetic rats: effects on insulin secretion and small bowel motility. *Neurogastroenterol Motil* **21**:313-321.

Gao W, Dai H, Knight DR, Calle R, Novartny M, Smith AH, Eskra JD, Preston GM and Jusko WJ (2007) Comparison of Two Insulin-Glucose Dynamic Models in Monkeys (Abstract). *AAPS Annual Meeting and Exposition, T 2473*.

Gibiansky L, Gibiansky E, Kakkar T and Ma P (2008) Approximations of the target-mediated drug disposition model and identifiability of model parameters. *J Pharmacokinet Pharmacodyn* **35**:573-591.

Goke R, Larsen PJ, Mikkelsen JD and Sheikh SP (1995) Identification of specific binding sites for glucagon-like peptide-1 on the posterior lobe of the rat pituitary. *Neuroendocrinology* **62**:130-134.

Goto Y, Suzuki K, Ono T, Sasaki M and Toyota T (1988) Development of diabetes in the non-obese NIDDM rat (GK rat). *Adv Exp Med Biol* **246**:29-31.

Greig NH, Holloway HW, De Ore KA, Jani D, Wang Y, Zhou J, Garant MJ and Egan JM (1999) Once daily injection of exendin-4 to diabetic mice achieves long-term beneficial effects on blood glucose concentrations. *Diabetologia* **42**:45-50.

Klonoff DC, Buse JB, Nielsen LL, Guan X, Bowlus CL, Holcombe JH, Wintle ME and Maggs DG (2008) Exenatide effects on diabetes, obesity, cardiovascular risk factors and hepatic biomarkers in patients with type 2 diabetes treated for at least 3 years. *Curr Med Res Opin* **24**:275-286.

Kolterman OG, Kim DD, Shen L, Ruggles JA, Nielsen LL, Fineman MS and Baron AD (2005) Pharmacokinetics, pharmacodynamics, and safety of exenatide in patients with type 2 diabetes mellitus. *Am J Health Syst Pharm* **62**:173-181.

Landersdorfer CB and Jusko WJ (2008) Pharmacokinetic/pharmacodynamic modelling in diabetes mellitus. *Clin Pharmacokinet* **47**:417-448.

Larsen PJ, Tang-Christensen M, Holst JJ and Orskov C (1997) Distribution of glucagon-like peptide-1 and other preproglucagon-derived peptides in the rat hypothalamus and brainstem. *Neuroscience* **77**:257-270.

Linnebjerg H, Kothare PA, Park S, Mace K, Reddy S, Mitchell M and Lins R (2007) Effect of renal impairment on the pharmacokinetics of exenatide. *Br J Clin Pharmacol* **64**:317-327.

Mager DE, Abernethy DR, Egan JM and Elahi D (2004) Exendin-4 pharmacodynamics: insights from the hyperglycemic clamp technique. *J Pharmacol Exp Ther* **311**:830-835.

Mager DE and Jusko WJ (2001) General pharmacokinetic model for drugs exhibiting target-mediated drug disposition. *J Pharmacokinet Pharmacodyn* **28**:507-532.

Mager DE, Wyska E and Jusko WJ (2003) Diversity of mechanism-based pharmacodynamic models. *Drug Metab Dispos* **31**:510-518.

Ohara-Imaizumi M, Nishiwaki C, Kikuta T, Nagai S, Nakamichi Y and Nagamatsu S (2004) TIRF imaging of docking and fusion of single insulin granule motion in primary rat pancreatic beta-cells: different behaviour of granule motion between normal and Goto-Kakizaki diabetic rat beta-cells. *Biochem J* **381**:13-18.

Parkes DG, Pittner R, Jodka C, Smith P and Young A (2001) Insulinotropic actions of exendin-4 and glucagon-like peptide-1 in vivo and in vitro. *Metabolism* **50**:583-589.

Perez-Tilve D, Gonzalez-Matias L, Aulinger BA, Alvarez-Crespo M, Gil-Lozano M, Alvarez E, Andrade-Olivie AM, Tschop MH, D'Alessio DA and Mallo F (2010) Exendin-4 increases blood glucose levels acutely in rats by activation of the sympathetic nervous system. *Am J Physiol Endocrinol Metab* **298**:E1088-1096.

Phillips A, Janssen U and Floege J (1999) Progression of diabetic nephropathy. Insights from cell culture studies and animal models. *Kidney Blood Press Res* **22**:81-97.

Sandoval DA, Bagnol D, Woods SC, D'Alessio DA and Seeley RJ (2008) Arcuate glucagon-like peptide 1 receptors regulate glucose homeostasis but not food intake. *Diabetes* **57**:2046-2054.

Sato N, Komatsu K and Kurumatani H (2003) Late onset of diabetic nephropathy in spontaneously diabetic GK rats. *Am J Nephrol* **23**:334-342.

Satoh F, Beak SA, Small CJ, Falzon M, Ghatei MA, Bloom SR and Smith DM (2000) Characterization of human and rat glucagon-like peptide-1 receptors in the neurointermediate lobe: lack of coupling to either stimulation or inhibition of adenylyl cyclase. *Endocrinology* **141**:1301-1309.

Schrijvers BF, De Vriese AS, Van de Voorde J, Rasch R, Lameire NH and Flyvbjerg A (2004) Long-term renal changes in the Goto-Kakizaki rat, a model of lean type 2 diabetes. *Nephrol Dial Transplant* **19**:1092-1097.

Sharma A, Ebling WF and Jusko WJ (1998) Precursor-dependent indirect pharmacodynamic response model for tolerance and rebound phenomena. *J Pharm Sci* **87**:1577-1584.

Silber HE, Jauslin PM, Frey N and Karlsson MO (2010) An integrated model for the glucose-insulin system. *Basic Clin Pharmacol Toxicol* **106**:189-194.

Simonsen L, Pilgaard S, Orskov C, Hartmann B, Holst JJ and Deacon CF (2009) Long-term exendin-4 treatment delays natural deterioration of glycaemic control in diabetic Goto-Kakizaki rats. *Diabetes Obes Metab* **11**:884-890.

Simonsen L, Pilgaard S, Orskov C, Rosenkilde MM, Hartmann B, Holst JJ and Deacon CF (2007) Exendin-4, but not dipeptidyl peptidase IV inhibition, increases small intestinal mass in GK rats. *Am J Physiol Gastrointest Liver Physiol* **293**:G288-295.

Tornehave D, Kristensen P, Romer J, Knudsen LB and Heller RS (2008) Expression of the GLP-1 receptor in mouse, rat, and human pancreas. *J Histochem Cytochem* **56**:841-851.

Tourrel C, Bailbe D, Lacorne M, Meile MJ, Kergoat M and Portha B (2002) Persistent improvement of type 2 diabetes in the Goto-Kakizaki rat model by expansion of the beta-cell mass during the prediabetic period with glucagon-like peptide-1 or exendin-4. *Diabetes* **51**:1443-1452.

Vahl TP, Tauchi M, Durler TS, Elfers EE, Fernandes TM, Bitner RD, Ellis KS, Woods SC, Seeley RJ, Herman JP and D'Alessio DA (2007) Glucagon-like peptide-1 (GLP-1)

receptors expressed on nerve terminals in the portal vein mediate the effects of endogenous GLP-1 on glucose tolerance in rats. *Endocrinology* **148**:4965-4973.

Widmann C, Dolci W and Thorens B (1995) Agonist-induced internalization and recycling of the glucagon-like peptide-1 receptor in transfected fibroblasts and in insulinomas. *Biochem J* **310 (Pt 1)**:203-214.

Xu G, Stoffers DA, Habener JF and Bonner-Weir S (1999) Exendin-4 stimulates both beta-cell replication and neogenesis, resulting in increased beta-cell mass and improved glucose tolerance in diabetic rats. *Diabetes* **48**:2270-2276.

Young AA, Gedulin BR, Bhavsar S, Bodkin N, Jodka C, Hansen B and Denaro M (1999) Glucose-lowering and insulin-sensitizing actions of exendin-4: studies in obese diabetic (ob/ob, db/db) mice, diabetic fatty Zucker rats, and diabetic rhesus monkeys (Macaca mulatta). *Diabetes* **48**:1026-1034.

Zheng D, Ionut V, Mooradian V, Stefanovski D and Bergman RN (2009) Exenatide sensitizes insulin-mediated whole-body glucose disposal and promotes uptake of exogenous glucose by the liver. *Diabetes* **58**:352-359.

Footnote

This work was supported by National Institutes of Health [Grants GM24211, GM57980].

Legends for figures.

Figure 1. The PK/PD model for exendin-4 in GK rats. Symbols are defined in the text and tables.

Figure 2. Exendin-4 concentration versus time profiles following single doses (0.5, 1, 5 and 10 μg/kg by iv injection and 5 μg/kg by sc injection in GK rats. Solid lines are fitted profiles.

Figure 3. Effect of exendin-4 doses on noncompartmental values of systemic clearance (*CL*), steady-state volume of distribution (V_{ss}), distributional clearance (CL_D), and initial volume of distribution (V_c) based on PK data.

Figure 4. Time profiles of insulin (left) and glucose (right) concentrations after single bolus administration of exendin-4 to GK rats at the indicated doses. Solid lines are fitted profiles.

Figure 5. Observed glucose and insulin concentrations in the confirmatory animal studies overlaid with model simulations. Symbols represent observations from individual rats, and lines are model predictions obtained by setting basal insulin and glucose concentrations (Ins_0 and Glu_0) as the mean values of each rat group.

Figure 6. Simulated time profiles of the exendin-4-GLP-1R complex (RC) from the TMDD model in GK rats.

Figure 7. Simulated time profiles of insulin and glucose from the PK/PD model in GK rats. Basal insulin and glucose concentrations (Ins_0 = 3.75 ng/ml and Glu_0 = 276 mg/dL) were the average values in all the rats.

JPET Fast Forward. Published on December 14, 2010 as DOI: 10.1124/jpet.110.175752
This article has not been copyedited and formatted. The final version may differ from this version.

Table 1. Parameter estimates obtained from the time profiles of exendin-4 following administration to GK rats with the TMDD PK model

Parameter	Definition	Estimate (CV%)
k_{el} (min^{-1})	Renal elimination rate constant	0.095 (14)
k_{pt} (min^{-1})	Intercompartmenal rate constant	0.067 (65)
k_{tp} (min^{-1})	Intercompartmenal rate constant	0.180 (38)
V_c (ml/kg)	Central volume of distribution	90.5 (16)
k_{on} (L/(nmol·min))	Second-order receptor binding rate constant	0.0794 (19)
k_{off} (min^{-1})	First-order dissociation rate constant	0.0150 (17)
k_{int} (min^{-1})	Internalization rate constant	0.00358 (35)
R_{tot} (nmol/L)	Receptor conc. at steady-state	5.17 (24)
k_{deg} (min^{-1})	GLP-1R degradation constant	0.0178 (28)
F	Bioavailability	0.507 (21)
k_a (min^{-1})	Absorption rate constant	0.0532 (10)
CLc (ml/kg/min)	Central clearance (k_{el} x V_c)	8.6[a]
K_D (nmol/L)	Equilibrium dissociation constant (k_{off} /k_{on})	0.19[a]

[a]Secondary parameter.

JPET Fast Forward. Published on December 14, 2010 as DOI: 10.1124/jpet.110.175752
This article has not been copyedited and formatted. The final version may differ from this version.

Table 2. Parameter estimates obtained from the insulin and glucose profiles after single bolus injection of exendin-4 to GK rats with the PK/PD model

Parameter	Definition	Estimate (CV%)
k_{outI} (min^{-1})	Insulin output rate constant	0.483 (36)
k_p (min^{-1})	Insulin precursor release rate constant	0.135 (13)
Ins_0 (ng/ml)	Basal Insulin (0.5, 1, 5, 10, 5 (sc) µg/kg)	2.82 (6), 3.66 (4), 2.83 (4), 3.06 (4), 3.71 (6)
Glu_0 (mg/dl)	Basal glucose (0.5, 1, 5, 10, 5 (sc) µg/kg)	330 (6), 280 (7), 245 (7), 197 (8), 262 (7)
k_{outG} (min^{-1})	Glucose output rate constant	0.0224 (48)
Ins_h (ng/ml)	Threshold insulin	1.44[a]
S_I (ml/ng)	Stimulation factor of insulin on glucose disposal	0.708 (42)
S_{max}	Maximum insulintropic response factor	6.91 (45)
SC_{50} (nmol/L)	Concentration for 50% of insulintropic effect	1.29 (73)
S_{RC} (L/nmol)	Stimulation factor on glucose production	0.112 (34)

[a]Parameter fixed as literature value.

Figure 1

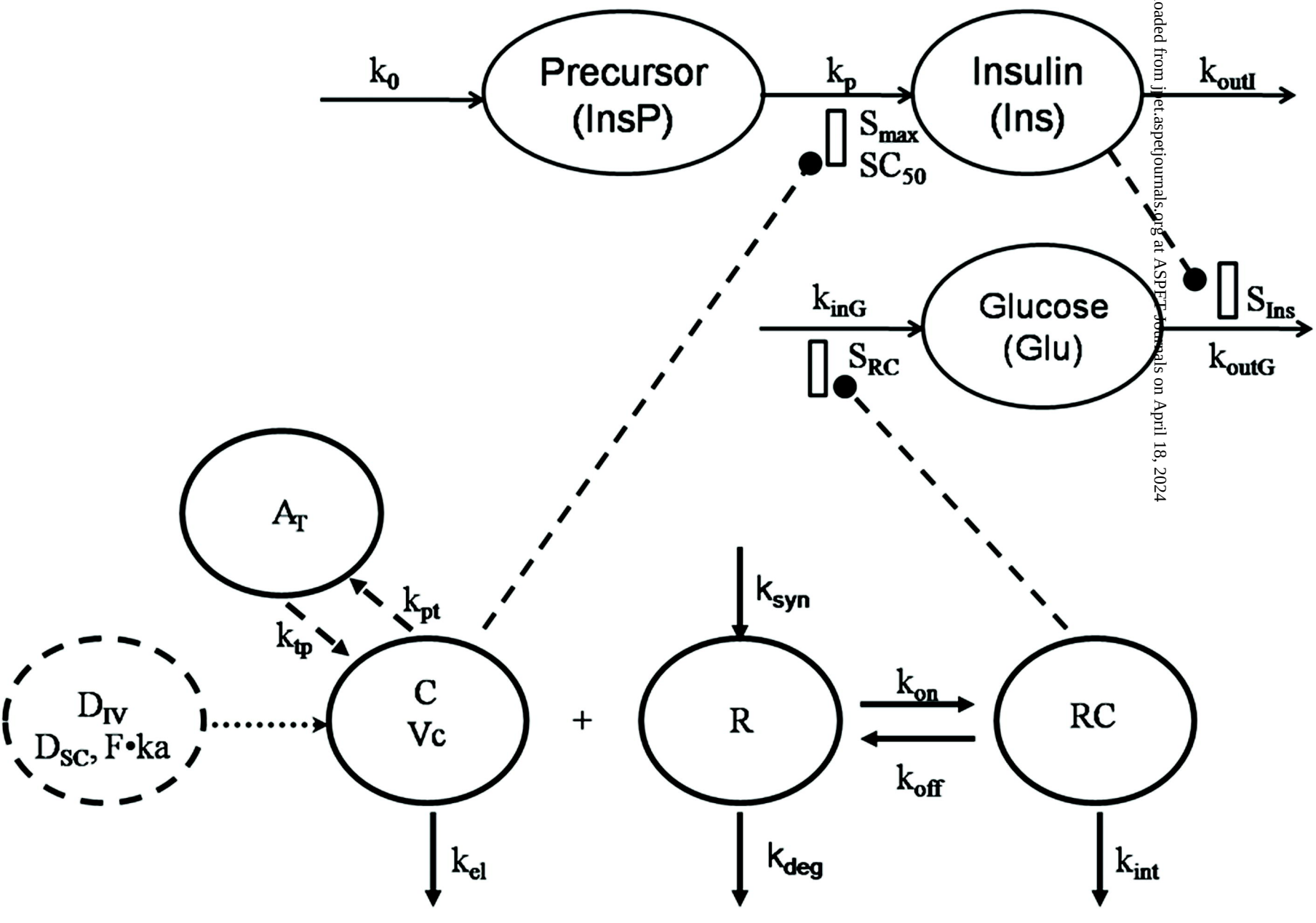

Figure 2

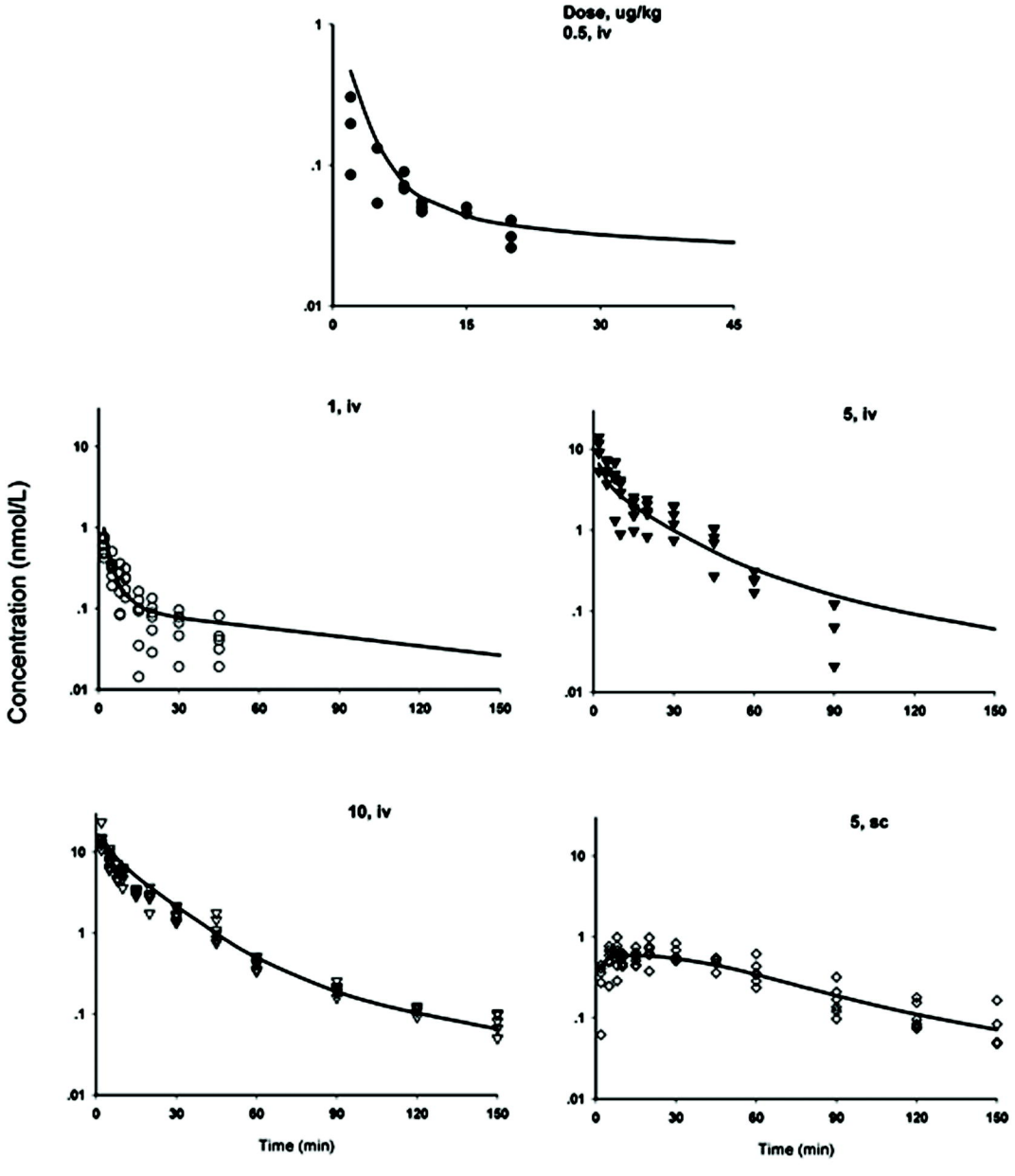
Dose, ug/kg
0.5, iv
1, iv
5, iv
10, iv
5, sc
Concentration (nmol/L)
Time (min)
Time (min)

Figure 3

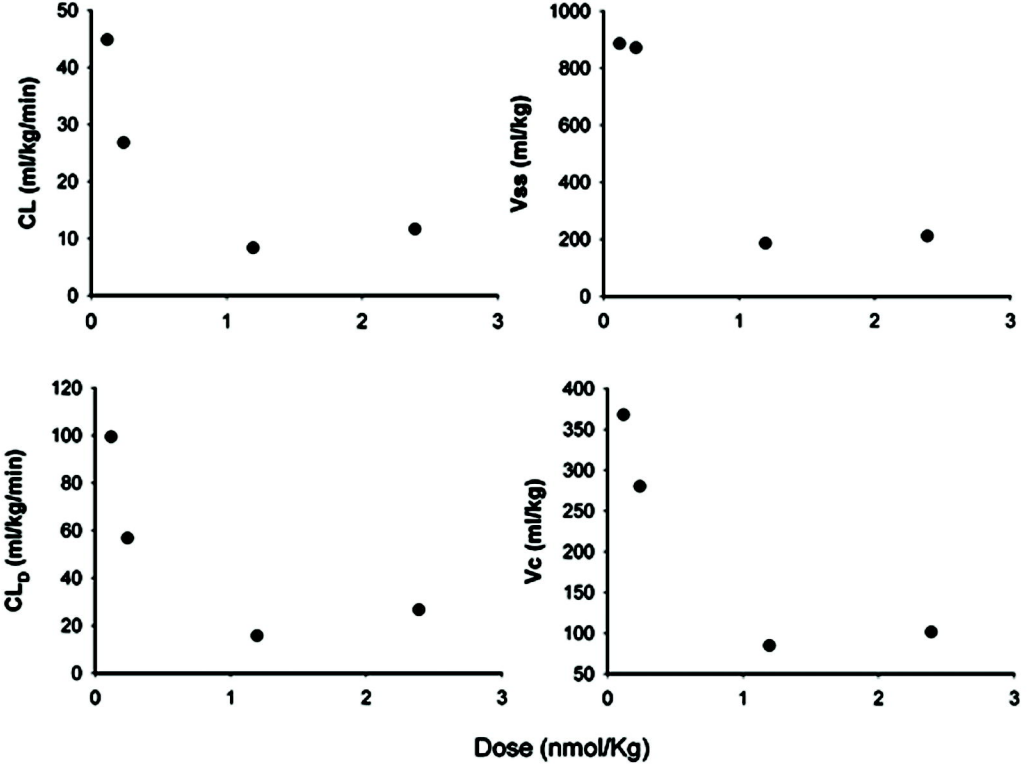

Figure 4

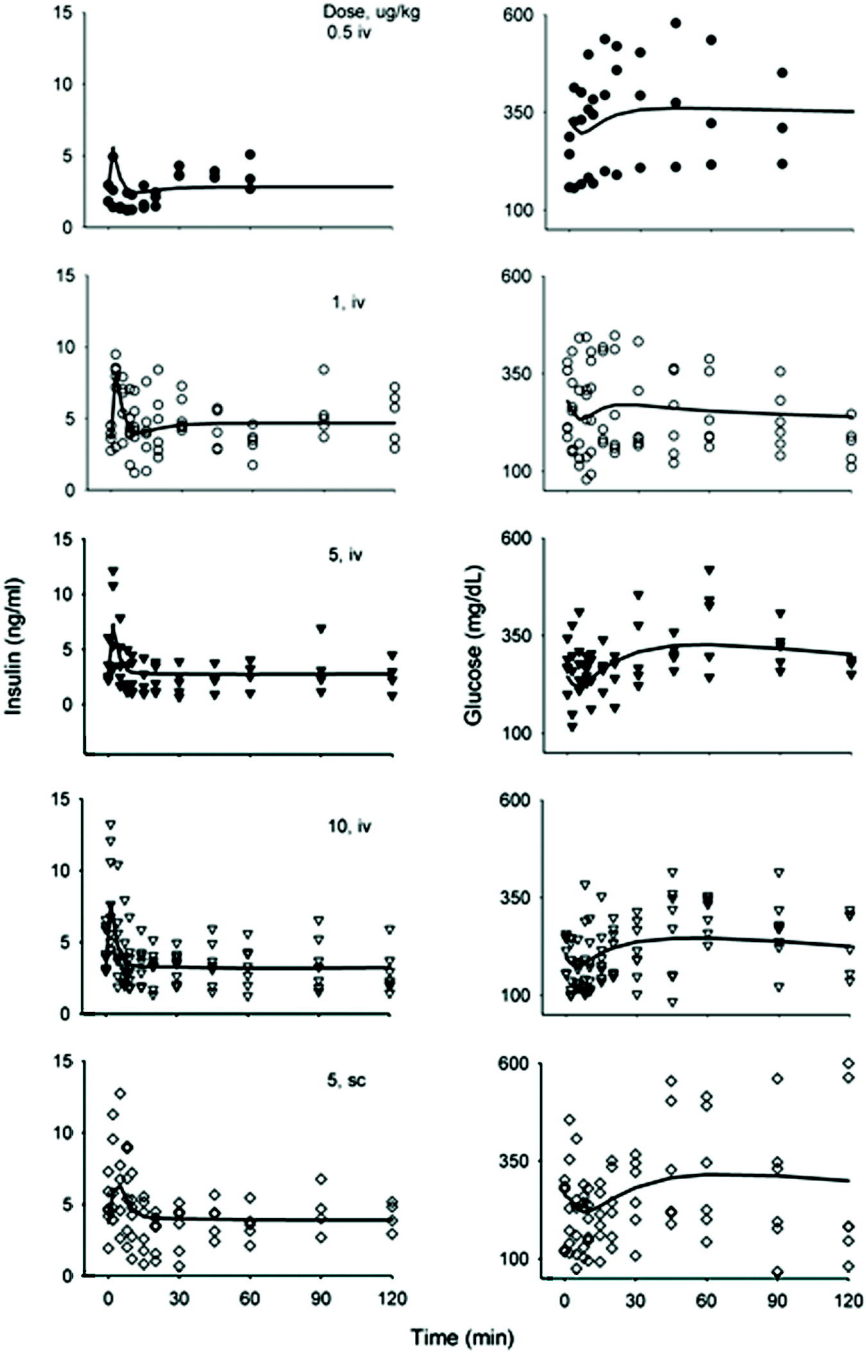
Dose, ug/kg
0.5 iv
1, iv
5, iv
10, iv
5, sc
Insulin (ng/ml)
Glucose (mg/dL)
Time (min)
0
30
60
90
120
0
5
10
15
100
350
600

Figure 5

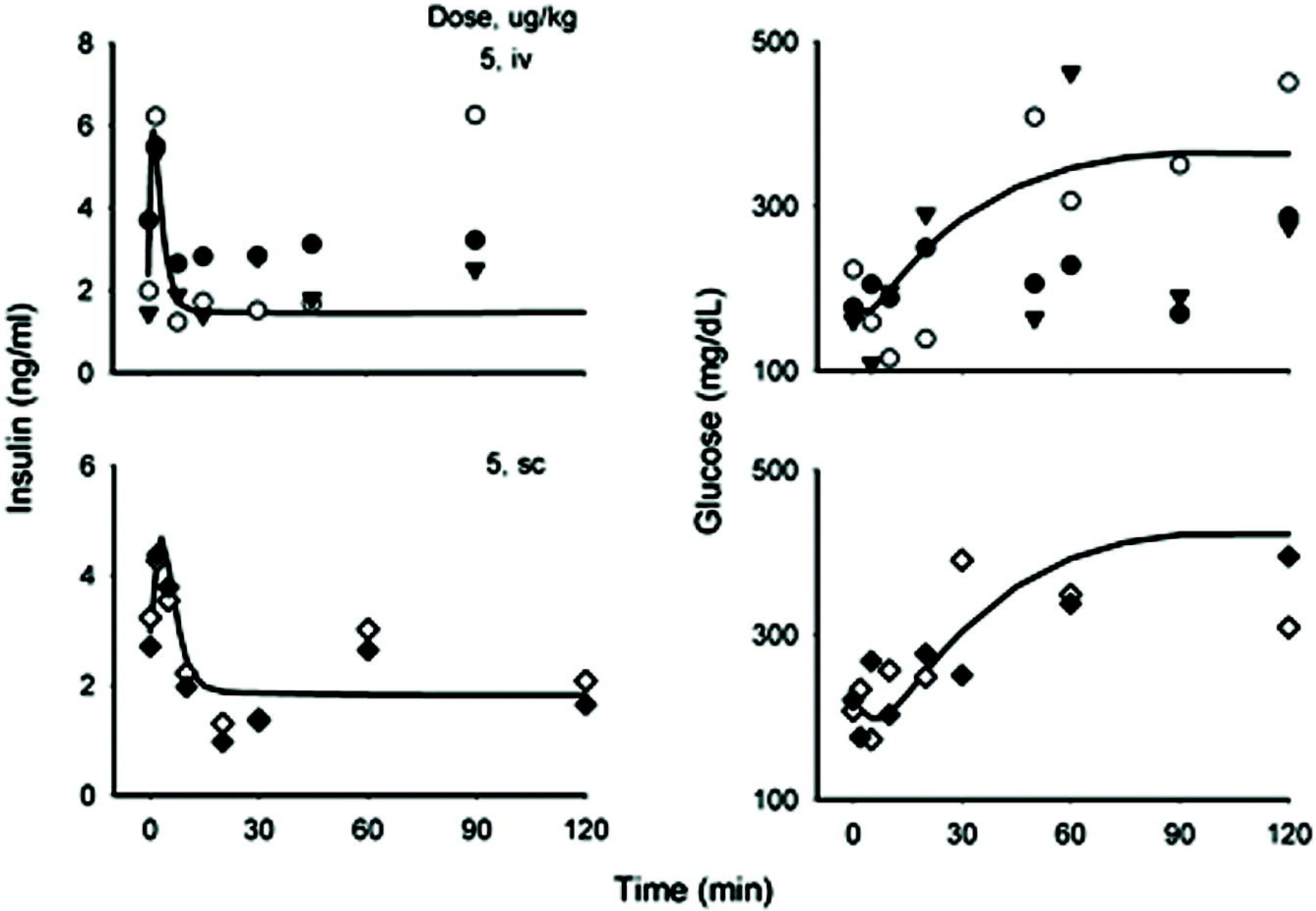
Dose, ug/kg
5, iv
5, sc
Insulin (ng/ml)
Glucose (mg/dL)
Time (min)
0
2
4
6
8
100
300
500
0
30
60
90
120

Figure 6

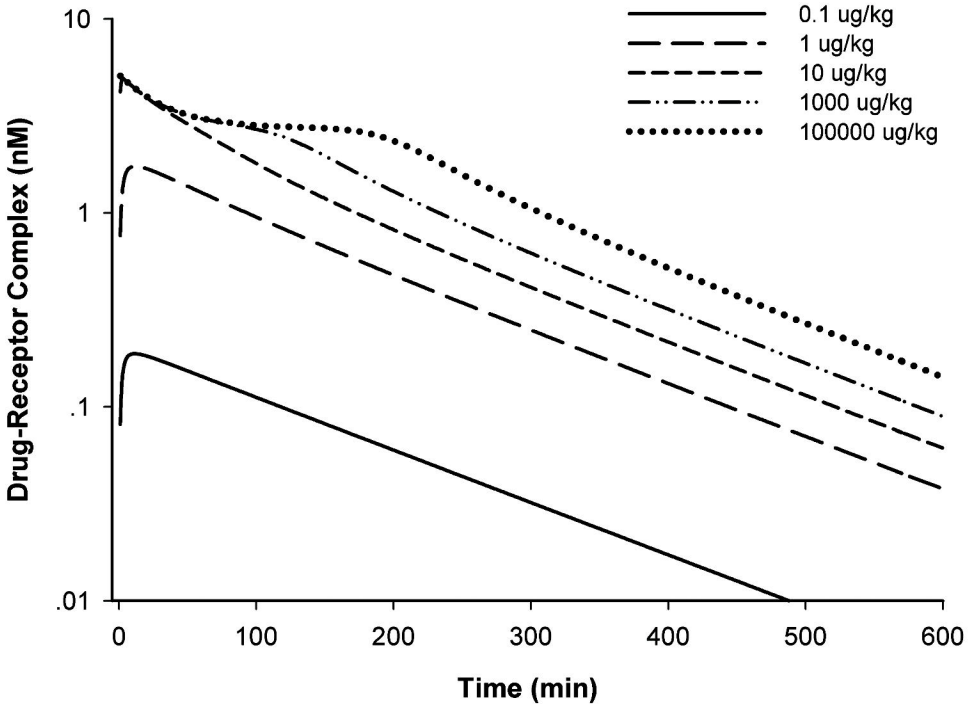
0.1 ug/kg
1 ug/kg
10 ug/kg
1000 ug/kg
100000 ug/kg
Drug-Receptor Complex (nM)
10
1
.1
.01
0
100
200
300
400
500
600
Time (min)

Figure 7

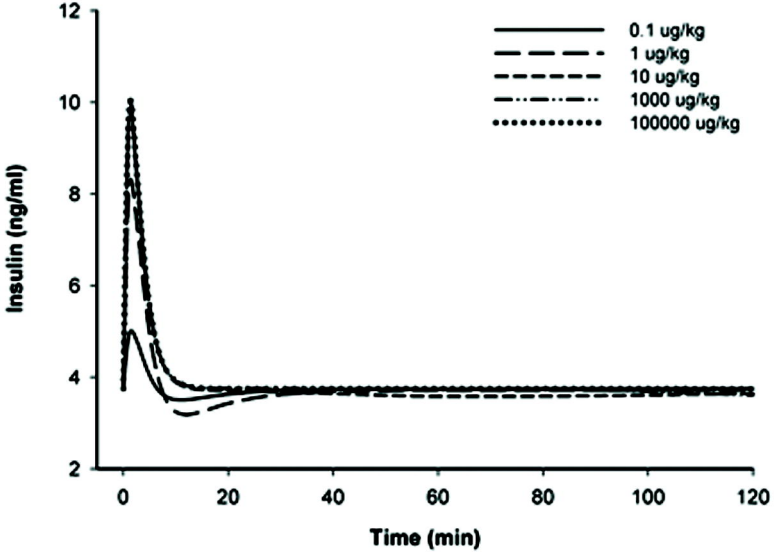
0.1 ug/kg
1 ug/kg
10 ug/kg
1000 ug/kg
100000 ug/kg
Insulin (ng/ml)
12
10
8
6
4
2
0
20
40
60
80
100
120
Time (min)

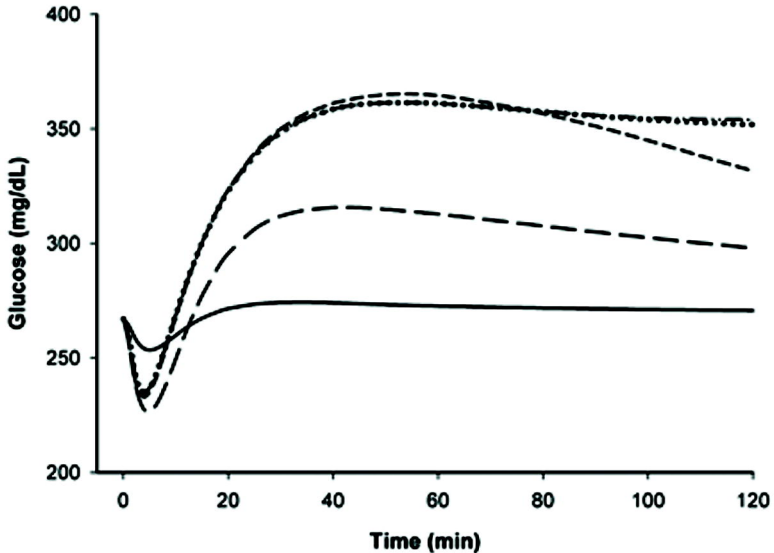
Glucose (mg/dL)
400
350
300
250
200
0
20
40
60
80
100
120
Time (min)